SYN-EXHUMATION PERVASIVE BRITTLE DEFORMATION IN THE VOLTRI (NW ITALY) SERPENTINITE: THE CHRYSOTILE-CEMENTED ACQUASANTA BRECCIA

Luca Barale*,°°, Fabrizio Piana*,°°,✉, Chiara Avataneo*,*, Serena Botta***, Giancarlo Capitani°, Roberto Cossio**, Igor Marcelli*,***, Jasmine Rita Petriglieri**,*,°°, Sergio Tallone*, Francesco Turci°°,°°°,*** and **Roberto Compagnoni**,°°**

* *Institute of Geosciences and Earth Resources, National Research Council of Italy, Torino, Italy*
** *Department of Earth Sciences, University of Torino, Italy.*
*** *Gi-RES srl, Torino, Italy.*
° *Dept. of Earth and Environmental Sciences (DISAT), University of Milano Bicocca, Italy.*
°° *"G. Scansetti" Interdepartmental Center for Studies on Asbestos and Other Toxic Particulates, University of Torino, Italy.*
°°° *Department of Chemistry, University of Torino, Italy*
✉ *Corresponding author, email: fabrizio.piana@cnr.it*

Keywords: *serpentinite; tectonic breccia; chrysotile: asbestos; NOA risk assessment; Voltri Massif; Italy.*

ABSTRACT

This paper sheds light on syn-exhumation, pervasive cataclastic processes occurred on competent serpentinites of a metaophiolitic sub-unit of the Voltri Massif. The reported data highlight the importance of the compositional and structural heterogeneities within the ophiolite-bearing exhumation channels, since the observed pervasive cataclastic processes affected only the more competent rock bodies of the metaophiolitic unit, giving origin to a serpentinite breccia, named as Acquasanta Breccia. This breccia is cemented by random-oriented chrysotile fibers that give rise to a very uncommon microstructure, as highlighted by optical microscopy, Micro-Raman spectroscopy, SEM-EDS and TEM investigations. The Acquasanta Breccia underwent a sequence of syn-exhumation tectonic events, accompanied by the onset of different generations and types of chrysotile, which occur both in veins and in the rock matrix. The breccia records the intermediate and late stages of the exhumation of the Voltri meta-ophiolites, which occurred after the development of the retrograde greenschist-facies foliation and before the late shallower faulting events.

INTRODUCTION

During a geological study in the Genoa (Genova) hinterland in NW Italy (Botta et al., 2020; Barale et al., 2020) focused to define a geo-environmental model supporting tunnel excavation in asbestos-bearing meta-ophiolites a peculiar and widespread serpentinite breccia was identified, not reported in the geologic literature. This breccia, briefly described in Botta et al. (2020), is formed by serpentinite clasts cemented by a brown material mainly consisting of chrysotile, identified only after a detail laboratory study, whose content may reach up to 50% of the rock by volume. This serpentinite breccia, here named Acquasanta Breccia, occurs within the Voltri tectono-metamorphic unit (Voltri Unit) of the 'Voltri Massif' tectono-metamorphic complex (Capponi and Crispini, 2008) (Fig. 1). The Acquasanta Breccia provides informations on some tectonic stages of the retrograde metamorphic evolution of the Voltri Unit that occurred during exhumation, after the onset of the Alpine eclogite-facies metamorphism.

The Acquasanta Breccia crops out between the Branega and Leira valleys (Fig. 2) close to the Acquasanta thermal spring site within the Acquasanta Lithotectonic Unit (**ALU**), a sub-unit of the Voltri Unit, here described for the first time. The ALU consists of an assemblage of different-order tectonic slices, bounded by two main tectonic contacts, among which the Acquasanta-type brecciated serpentinite is largely represented.

The study of the Acquasanta Breccia contributes to shed light on the serpentinization and serpentine precipitation processes, and related deformational mechanisms, that occur at relatively shallow crustal levels (e.g., Andreani et al., 2005; Hirauchi, 2006; Hirauchi and Yamaguchi, 2007) and even in ultramafite-derived clastic sedimentary deposits (Cashman and Whetten, 1976; Craw et al., 1987; Barale et al., 2022). In this study case, a widespread precipitation of serpentine occurred after the main retrograde tectono-metamorphic events and could allow a better understanding of the deformation-related serpentinization processes that occur at shallow depth not only along late faults and fractures, but extensively within large rock volumes, as also reported by Hirauchi (2006) for a different study case in California.

Furthermore, as the cataclastic processes that originated the Acquasanta Breccia seem to be developed only into the more competent rock bodies of the Voltri Unit meta-ophiolitic complex (massive serpentinites and serpeninized peridotites), it could be of interest for a wider discussion about the role of the lithological and structural heterogeneities in the exhumation channel dynamics (e.g., Guillot et al., 2009; Festa et al., 2010; 2019; Malatesta et al., 2012).

Finally, the present paper gives a contribution to discriminate between the several types of serpentinite breccia that characterize the Voltri Massif, which seems to be coated by breccias of different type and nature, namely (i) tectonic breccias, (ii) fractured and variably weathered serpentinites and peridotites, and (iii) continental sedimentary breccias of different ages formed at the expense of (i) and (ii). All these lithotypes are, in several cases, hard to be distinguished from each other in the field, as already known since the pioneer works of Sacco (1889-1890) and Rovereto (1939). This could be explained not only because of their similar compo-

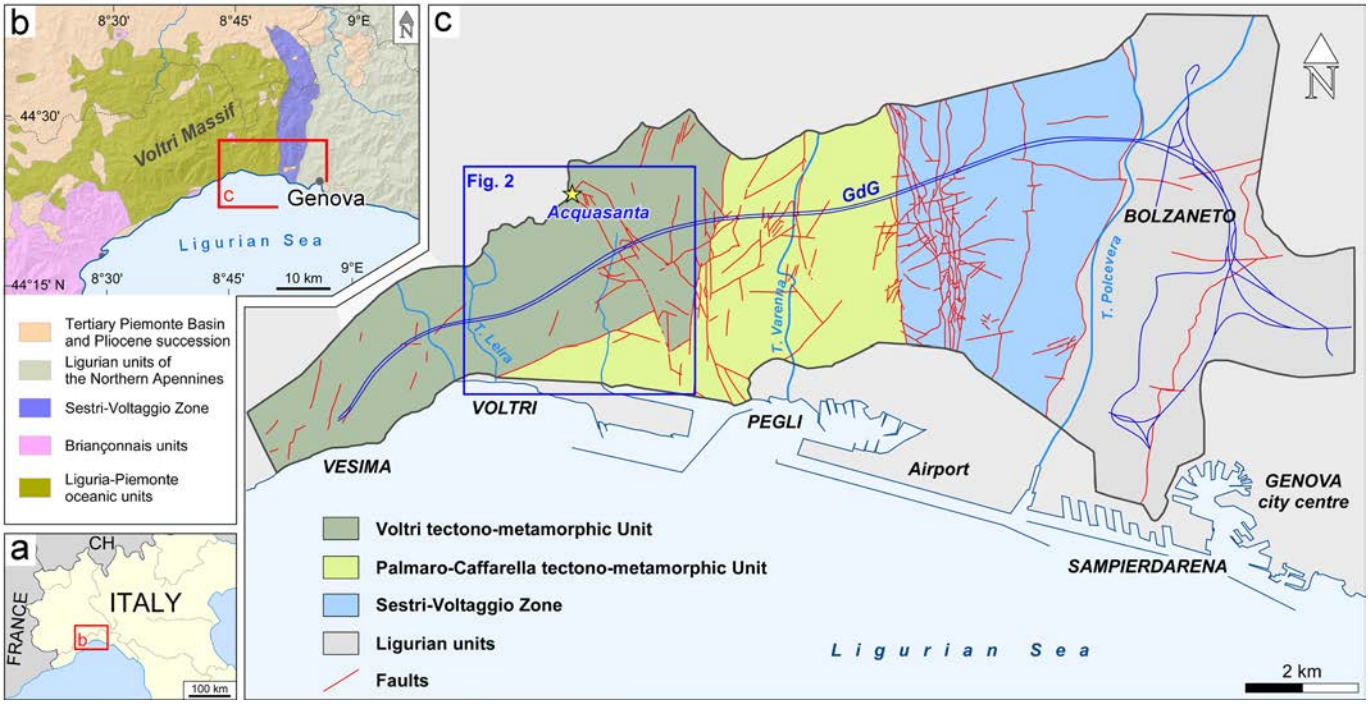

Fig. 1 - a) Location of the Genova area in NW Italy. b) Simplified geotectonic scheme of central Liguria with the meta-ophiolites of the "Voltri Massif" in the center. c) More detailed geotectonic scheme of the Genoa area. GdG: Gronda di Genova layout. Modified from Botta et al., 2020. The reader is referred to the PDF online for a colour version.

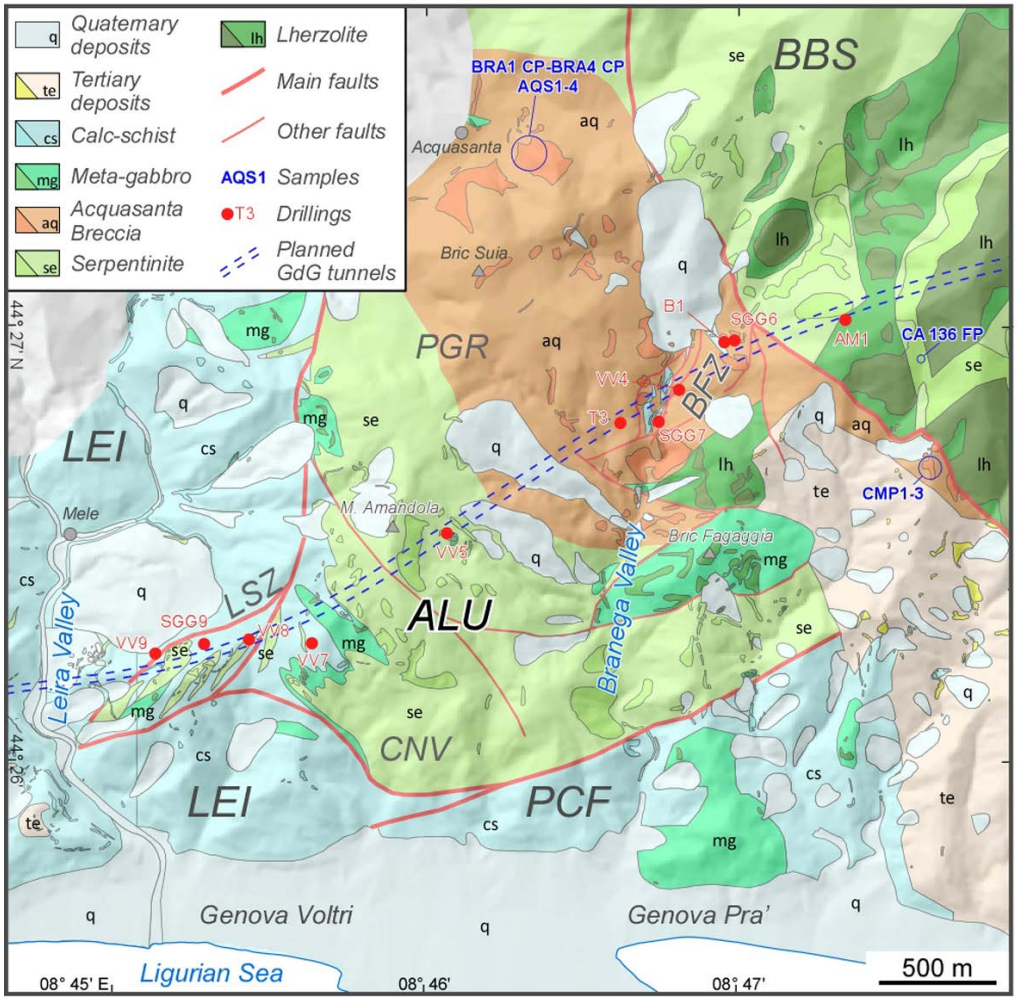

Fig. 2 - Geological map of the eastern part of Voltri Unit (location in Fig. 1). LEI: Leira Unit; ALU: Acquasanta Lithotectonic Unit; CNV: Canova sub-unit; PGR: Pian Grande sub-unit; BBS: Bric Boessa Unit; PCF: Palmaro-Caffarella Tectono-metamorphic Unit; LSZ: Leira Shear Zone; BFZ: Branega Fault Zone. The dashed blue lines indicate the layout of the Gronda di Genova (GdG) tunnels (see section in Fig. 3). Red dots: locations of the drilling sites; blue circle: location of the sampled outcrops.

sition, but also because serpentinization processes may have occurred at different times throughout the tectonic, erosional and depositional stages.

MATERIALS AND METHODS

Field work

A geological survey at scale 1:5,000 of the Acquasanta area was carried out in the years 2010-2017 in the framework of geoenvironmental studies related to the GdG highway tunnel system (see above). The portion of the new geological map relevant the ALU is shown in Fig. 2. A detailed structural analysis defined some homogeneous structural domains (lithotectonic units and sub-units) and macroscale structures, as well as the mesoscale structural features of the main lithotypes, the Acquasanta Breccia included. This study could also rely on the analysis of many drill cores and logs carried out for the GdG project. The integration of field data with drill core data allowed new reliable geological sections at 1:5000 scale to be made along the planned layout of the GdG tunnels: The geological section crossing the Acquasanta Breccia along the northern tunnel of the GdG is shown in Fig. 3.

Petrographic and mineralogical analyses

Twelve representative samples were collected from different points of the Acquasanta Unit (Table 1; Fig. 2). For each sample, a polished thin section (30 μm thick) was prepared and studied by means of optical polarized light microscopy (OM) with a Leica polarizing microscope DM750P, equipped with an Olympus BX41 photomicroscope.

OM observations were coupled with micro-Raman spectroscopy (μ-R) that is the only analytical technique suited for a rapid identification of serpentine minerals (Rinaudo et al. 2003; Groppo et al. 2006; Petriglieri et al., 2014; Compagnoni et al., 2021). Micro-Raman spectra were acquired at Dept. of Earth Sciences, University of Turin, using a Horiba-Jobin Yvon HR800 LabRAM instrument, equipped with a Nd-YAG laser (532 nm) 8mW power, an Olympus BX 40 optical microscope and a detector CCD cooled to -70°C by Peltier effect. The analytical conditions were: 200 μm confocal hole, 100X objective lens (1 μm lateral spatial resolution), 1 cm^{-1} spectral resolution using 600 l/mm grid, 10 s and 10 reps. acquisition time on each spectrum. Correct calibration of the instrument was verified by checking the position of the Si band at 520.7 cm^{-1}. Spectra were processed using the Labspec 5 acquisition software. Spectra of serpentine minerals

Table 1 - List of the studied Acquasanta Breccia samples with geographical coordinates, pertaining Lithotectonic Units and indication of the analyses performed.

Sample	Coordinates	Lithotectonic Unit	OM	μ-R	SEM-EDS
AQS1	44°27'27.5"N; 8°46'21.3"E	Acquasanta Unit, Pian Grande sub-unit	x	x	
AQS2	44°27'27.5"N; 8°46'21.3"E	Acquasanta Unit, Pian Grande sub-unit	x	x	
AQS3	44°27'27.9"N; 8°46'20.4"E	Acquasanta Unit, Pian Grande sub-unit	x	x	
AQS4	44°27'27.9"N; 8°46'20.4"E	Acquasanta Unit, Pian Grande sub-unit	x	x	
CMP1	44°26'43.1"N; 8°47'35.9" E	Acquasanta Unit, Pian Grande sub-unit	x	x	
CMP2	44°26'43.1"N; 8°47'35.9" E	Acquasanta Unit, Pian Grande sub-unit	x	x	
CMP3	44°26'43.1"N; 8°47'35.9" E	Acquasanta Unit, Pian Grande sub-unit	x	x	
BRA1 CP	44°27'28.1"N; 8°46'19.7"E	Acquasanta Unit, Pian Grande sub-unit	x	x	
BRA2 CP	44°27'27.5"N; 8°46'21.1"E	Acquasanta Unit, Pian Grande sub-unit	x	x	x
BRA3 CP	44°27'27.2"N; 8°46'22.5"E	Acquasanta Unit, Pian Grande sub-unit	x	x	x
BRA4 CP	44°27'27.2"N; 8°46'22.5"E	Acquasanta Unit, Pian Grande sub-unit	x	x	x
CA136 FP	44°26'57.8"N 8°47'34.9"E	Bric Boessa Unit	x	x	x

Before TEM observation the mounts were carbon-coated to avoid electrostatic charging.

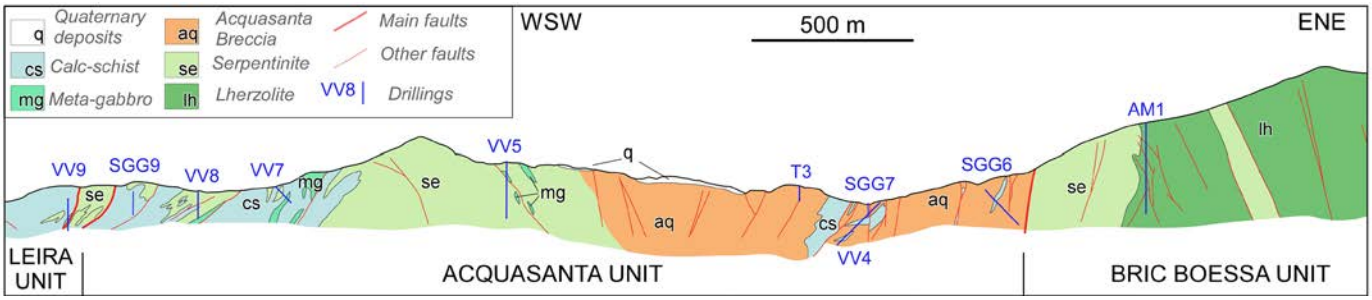

Fig. 3 - Geological cross-section through the eastern part of Voltri Unit, including the Leira, Acquasanta and Bric Boessa lithotectonic units. The cross-section is along the layout of the southern tunnel of the Gronda di Genova shown in Fig. 2. Drillings adjacent to the geological cross-section plane are projected on it.

were collected in the range 70-4000 cm^{-1}, to include also the most significant OH-stretching vibrations.

Quantitative analyses of the serpentine minerals were performed on selected thin sections by means of Scanning Electron Microscopy (SEM) coupled with Energy Dispersive Spectroscopy (EDS), using a JEOL JSM IT300LV Scanning Electron Microscope with W source, equipped with an EDS Oxford INCA Energy 200 at the Dept. of Earth Sciences, University of Torino. SEM-EDS analyses were made on carbon-coated thin sections, selected among the 12 samples studied by means of OM. The operating conditions were: 30 s counting time, 15 kV accelerating voltage, 10 mm working distance and 5 nA probe current. The collected data were processed with the Microanalysis Suite Issue 18c, INCA Suite Version 4.14. Morphological images of the chrysotile cement were obtained with the SEM by secondary electron (SE) imaging on carbon-coated rock fragments obtained by mechanical crushing; the images were acquired at 20 kV and 100 pA.

Transmission Electron Microscopy (TEM) investigations on a representative sample of the Acquasanta Breccia were undertaken by means of a JEOL JEM 2010 and of a JEOL JEM 2100P installed at the Dept. of Physical Sciences, Earth and Environment (DISFTA) of the University of Siena and at the Platform of Microscopy of the University of Milano-Bicocca (PMiB), respectively. Both instruments operate at 200 kV and both are equipped with a digital camera for image acquisition and an EDS system for chemical analyses. TEM mounts were prepared at the DISFTA by ion milling 3 mm wide disks selected on a double polished petrographic thin section with a Gatan Precision Ion Polishing System (PIPS). Before removing the disks from the thin section and ion-milling, a 3 mm wide Cu-ring with an internal hole of 1 mm was glued on the areas of interest. Before TEM observations the mounts were carbon-coated to avoid electrostatic charging.

GEOLOGICAL SETTING

Regional geological setting

The study area is located in the Ligurian Alps (Genova hinterland) (Fig. 1) and includes the "Voltri Massif" a metamorphic complex consisting of middle Jurassic-early Cretaceous meta-ophiolites and metasediments (Chiesa et al., 1975; Vanossi et al., 1984) derived from the Liguria-Piemonte oceanic domain (Bernoulli et al., 1979).

The Voltri Massif consists of rocks affected by Alpine eclogite-facies metamorphism (Federico et al., 2004). This high-pressure (HP) metamorphic overprint occurred during the subduction-connected the early collisional Alpine tectonic stages (middle-late Eocene, 49-46 Ma) (Rubatto and Scambelluri, 2003; Federico et al., 2005). The HP mineral assemblages were partially re-equilibrated under greenschist-facies conditions connected to the late Eocene-early Oligocene exhumation of the Ligurian Alps (Hoogerduijn Strating, 1994; Federico et al., 2005; Vignaroli et al., 2008; 2010). This retrograde tectono-metamorphic evolution could have occurred during a complex extensional setting at the Alps-Apennines crustal junction, characterized by two opposite-verging subduction zones (see discussion in Vignaroli et al. (2009, with references therein).

In this paper, which concerns the southern part of the Voltri Massif, is intended as "Voltri Unit" (Fig. 1) a tectono-metamorphic unit made up of the meta-ophiolites and metasediments (Turchino calc-schists), partially corresponding to the Voltri-Rossiglione Unit *sensu* Chiesa et al. (1975) and Vignaroli et al. (2010) in the southern part of the Voltri Massif.

The Voltri Unit is in contact to the East and to the South with the Palmaro-Caffarella tectono-metamorphic Unit (Capponi and Crispini, 2008) (Figs. 1 and 3), which consists of the same lithotypes but affected by blueschist-facies metamorphism (e.g., Chiesa et al., 1975; Capponi et al., 2016), (middle Eocene in age, 43-41 Ma, Federico et al., 2005); to the South, the Voltri Unit is in contact with a composite tectonic slice zone known as Sestri-Voltaggio Zone (Cortesogno and Haccard, 1984; Crispini and Capponi, 2001). This zone consists of several tectonic sub-units (Gazzo-Isoverde, Cravasco-Voltaggio and Figogna units) made of metasedimentary and metaophiolite rocks showing variable degrees of metamorphic transformation, ranging from very low grade to high pressure metamorphism.

Local geological setting

The above setting has been analyzed at a greater detail during the field work, with the aim to separate the study area into homogeneous lithotectonic sub-units. These subdivisions, originally thought with the aim to address the asbestos risk assessment (Botta et al., 2020) within and across a number of relatively homogeneous domains, are proposed also in this paper, as sectors characterized by one or two recurrent lithotypes and a relatively constant structural setting or structural associations. For instance, the damaged zones along the main faults have been separated from the tectonic slice zones, as well as from other tectonic units dominated by folds, or again from units consisting of constantly dipping fold-flank zones. Each sub-unit is bounded by a fault or a shear zone cutting the main syn-greenschist - facies regional foliation.

In this way, a number of post-metamorphic lithotectonic units were individuated within the study area of the Voltri and Palmaro-Caffarella main tectono-metamorphic units, which are reported in Fig. 3, namely the Acquasanta Lithotectonic Unit (ALU) with the Pian Grande and Canova internal minor units, the Leira Shear Zone (LSZ), the Branega Fault Zone (BFZ), the Bric Boessa (BBS) and Leira (LEI) tectonic units.

The Acquasanta Lithotectonic Unit (ALU)

ALU is located in the southeastern part of the Voltri Unit (Figs. 1 and 2) and is largely represented by the Acquasanta Breccia (Figs. 3 and 4). The ALU extends for about five square kilometers from the eastern flank of the Branega Valley to the East, toward the Acquasanta sector to the West (Fig. 2). The ALU structural setting is given by two main, km-scale tectonic contacts. The upper one, LSZ, separates it from the Turchino calc-schists of the Leira Unit and the lower one - here referred to as BFZ - from the meta-ophiolites of the Bric Boessa Tectonic Unit (Fig. 2).

The LSZ is a ductile to brittle shear zone that separates a number of interlayered hundred-meters sized slices of calc-schists, metagabbros and foliated serpentinites from the main serpentinite body of the Canova tectonic sub-unit (Fig. 2). The LSZ formed since the early stages of the retrograde metamorphic evolution, during which different lithotypes were folded and sheared under ductile to semi-brittle conditions. Although intensively reactivated during the late tectonic stages, as indicated by a diffuse cataclastic deformation affecting the serpentinite slices and the development of fault breccia along discrete tectonic slip surfaces, the LSZ partially preserves the original setting of a ductile, syn-greenschist - facies metamorphic shear zone, developed in a contractional tectonic regime coeval or slightly post-dating the relevant folding events.

Conversely, in the ALU footwall, the BFZ appears to be a deformation unit mostly characterized by fault-related frictional processes. The BFZ is hundred-meter-thick and involves several slices of serpentinite and calc-schist: It developed mostly under brittle regime, as indicated by the dominant cataclastic fabric (Fig. 5e, f) of fault rocks along the contacts between the repeated slices of serpentinites and calc-schists, found in the Branega Valley subsurface, down to the depth of at least 150 meters (see drill hole B1 and SGG6 logs, Fig. 6, available by courtesy of ASPI, Autostrade per l'Italia SpA). Although reliable kinematic indicators are scarce within the BFZ, the overall geometry and internal mesoscale structures point for a transpressional kinematics, later and partially reactivated by extensional faulting, with normal to oblique slip directions.

The ALU consists of tectonic slices of metabasites, calc-schists, micaschists and massive or brecciated serpentinites. It can be subdivided into two sub-units (Fig. 2): The northern Pian Grande sub-unit (PGR), and the southern Canova sub-unit (CNV), separated by post-metamorphic faults, belonging to a ENE-WSW mainly strike-slip fault system and a NW-SE mainly transtensional fault system. The PGR sub-unit is mainly made of serpentinites, a large part of which - about two square kilometres - consists of the Acquasanta breccia lithotype. Approaching the eastern boundary of ALU, the Acquasanta breccia becomes progressively affected by a cataclastic fabric connected to the late shear deformation that occurred along the BFZ. The BFZ-related deformation caused the Acquasanta coarse-grained brecciated fabric to turn into a cataclastic flow structure and then to a fine-grained cataclasite or cataclastic breccia (Fig. 5e, f). Conversely, the CNV sub-unit is characterized by massive serpentinites, with very few interlayers of the Acquasanta breccia lithotype, localized in its western part, and metabasite in the eastern one. The CNV sub-unit is bounded to the south by a ENE striking tectonic contact that is the southern tectonic boundary of the Voltri Unit, separating it from the Palmaro-Caffarella tectono-metamorphic unit.

THE ACQUASANTA BRECCIA

Mesoscale features

The Acquasanta Breccia is a well cemented tectonic breccia, which can be defined as a protocataclasite, namely a "non-foliated crackle-to-mosaic breccia" *sensu* Woodcock and Mort (2008). It is very compact and composed of heterometric serpentinite clasts, up to about half a meter across, usually angular or subangular in shape, and cemented by abundant fine-grained, dark green/blackish or red-brownish material (Figs. 4 and 5).

The Acquasanta Breccia underwent a partial internal reorganization by dm- to meter-spaced semi-brittle shear zones, which induced the development of dm-thick foliated portions. The whole breccia body is cut by discrete faults, marked by the development of fault rocks up to ca. ten cm thick.

The Acquasanta Breccia is also cut by several generations of mineral veins - from less than one mm to several mm-thick - filled with chrysotile and carbonate. The serpentine veins (generally very fragmented) are mostly older than brecciation, whereas carbonate veins are younger because systematically cutting across both the breccia clasts and the cement/matrix (Fig. 5f).

Microscopic characterization

For its distinctive and unusual characters, the Acquasanta Breccia was studied in detail to understand both the microscale processes that led to its formation, and the reasons of its anomalous behaviour regarding the asbestos release during rock grinding reported by Botta et al. (2020).

Optical microscopy

The Acquasanta Breccia mostly consists of antigorite serpentinite fragments, usually angular or subangular in shape, which are included in a yellowish-brownish cement, optically

Fig. 4 - Overall aspect of the Acquasanta breccia at the outcrop scale.

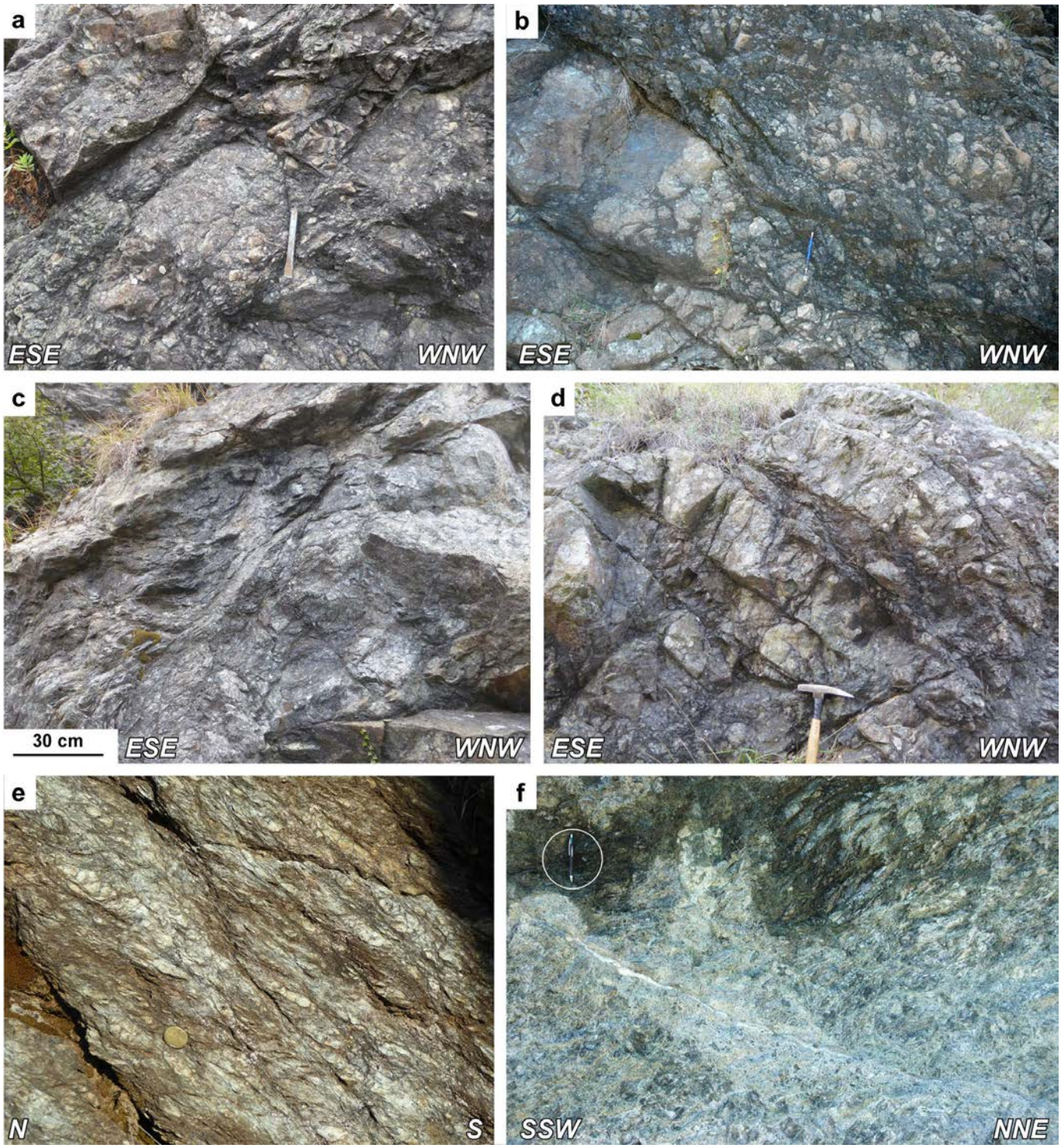

Fig. 5 - Field appearance of the Acquasanta breccia. a, b) cm- to dm-sized, light-brown serpentinite clasts homogeneously dispersed in a fine-grained dark-brownish matrix; c, d) two outcrops where the Acquasanta Breccia is cut by localized shear zones and later sets of faults; e, f) the most deformed portions of the rock mass showing a marked reorientation through cataclastic flow (e) and/or diffuse cataclasis of the primary Acquasanta Breccia clasts (f); "f " refers to the core of the Branega Fault Zone, BFZ. The scales are shown by the hammers in a) to d), by coin in e) and by the circled pen in f).

indeterminable, associated with opaque ore (Fig. 7a to f). Micro-Raman spectroscopy analyses (see below) revealed that this cement is mainly composed of chrysotile (Ctl2).

The antigorite serpentinite fragments show a number of microstructures including deformed interlocking, interpenetrated or foliated. However, pseudomorphs after primary mantle orthopyroxene ('bastite') and primary mantle clinopyroxene (locally with a very corroded appearance) are preserved in the less deformed samples. The ratio between cement and serpentinite clasts is greatly variable, and in some domains the cement may be volumetrically dominant. However, on average, the cement is about 20-30% of the rock by volume.

Thin chrysotile veins (Ctl 1) are present as clasts or within clasts of antigorite serpentinite where they are abruptly cut at clast edge (Fig. 8c, d), which indicates that they are older than

Fig. 6 - Core samples resulting from drilling in the Branega Fault Zone. a) Core samples of drill hole B1 taken at depth between 60 and 65 metres in the Branega Valley: at about 62.30 m depth, foliated cataclastic calc-schists make a transition to the underlying brecciated serpentinites (Acquasanta breccia); b) Core samples of drill hole SGG6 taken at depth between 80 and 85 metres: a calc-schist tectonic breccia and a gouge underlie brecciated serpentinites.

the brecciation event. The same is true for antigorite veins, either found within antigorite serpentinite clasts and interrupted at clast edges, or as vein fragments within the breccia (Fig. 8e, f).

Veins younger than the brecciation event, systematically cutting across both clasts and cement, are also observed (Fig. 7g, h). They are filled with both "slip" and "cross" chrysotile (Ctl 3; Fig. 8g) and rare lizardite, or with calcite/dolomite (Fig. 8h).

Micro-Raman spectroscopy

The several dozen micro-Raman analyses carried out on both cement and clasts of different thin sections document that the optically indeterminable yellowish-brownish cement systematically gives patterns characteristic of chrysotile (Fig. 9b) mixed with minor polygonal serpentines PS-15 (Fig. 9a) and PS-30 (Fig. 9c) (cf. Groppo et al., 2006; Compagnoni et al., 2021). In fact, within the experimental error, vibrations at around 1105 and 3698 cm^{-1}, typical of chrysotile and PS-15, are evident in all four spectra (Fig. 9a). The vibration at 691 cm^{-1} is closer to that of PS-15 than to the equivalent one of Ctl (Compagnoni et al., 2021). The 3698 cm^{-1} peak, which occurs in the vibrational field of OH, is very strong and flanked by a shoulder near 3685 cm^{-1} typical of PS-15 (Compagnoni et al., 2021). Conversely, the spectrum of late vein chrysotile (Fig. 9b) is typical of pure chrysotile with a higher degree of crystallinity as suggested by best peak/ background ratio. The PS-30 was identified for the peaks that systematically occur in the high-wavenumber region: the strongest peak at 3684 cm^{-1}, a shoulder at 3690 cm^{-1}, a minor peak at 3698 and a still lower peak at 3706 cm^{-1} (Fig. 9c).

As regards to serpentinite clasts, all serpentine phases, optically recognized as antigorite, consistently give the micro-Raman spectra of this mineral, which is characterized by a relatively small but sharp peak at around 1045 cm^{-1}, and two strong peaks in the vibrational field of (OH)-groups at 3670 e 3700 cm^{-1}, spaced approx. 30 cm^{-1} (Fig. 10a). The low-birefringence serpentine phase observed as pseudomorphs included in antigorite resulted to be lizardite. In the high- wavelength region the micro-Raman spectrum is characterized by two well defined peaks at around 3683 and 3704 cm^{-1}, spaced approx. 20 cm^{-1} (Fig. 10b).

In conclusion, the serpentine mineral of the clasts is systematically antigorite. Only a few lizardite aggregates, preserved in the core of some antigorite pseudomorphs after mantle clinopyroxene, were found in poorly deformed serpentinites and interpreted as relics of an early hydrothermal alteration. In some areas (samples CMP 1-3), abundant brownish fragments were observed among clasts. They include massive bundles of fibrous chrysotile (Fig. 8d), whereas the brownish, optically indeterminable, cement consists mainly of chrysotile (Ctl 2), polygonal serpentines PS-15 and PS-30, very minor opaque ores (magnetite, haematite, and possibly iron hydroxides, their hydration products), and rare small antigorite fragments. It is noteworthy that the nature of the yellowish to brownish-staining phases has not been identified, most likely because either too scarce to be detected and/or lost during sample preparation.

Scanning electron microscopy and EDS analyses

The secondary electron (SE) images (Fig. 11a, b) show that the material filling the space among the serpentinite clasts consists of thick and massive bundles of deformed fibres.

Several hundred SEM-EDS analyses were carried out on fibrous serpentine, antigorite of serpentinite clasts and on chrysotile of late - post-brecciation - veins. The antigorite of serpentinite clasts shows low contents of Al_2O_3 (~ 1 to ~ 3 wt%) and FeO (~ 2 to ~ 4 wt%) with traces of Cr and Ni. The fibrous serpentine is Al_2O_3–free and locally shows low concentrations of Ni and Cr. However, its wide range of FeO content (up to 12 wt%) suggests a probable submicroscopic mixture with Fe-oxides (magnetite and/or haematite). Furthermore, the common presence of Ca, an ion incompatible with the serpentine crystal structure, indicates a submicroscopic mixture with a Ca-bearing phase, most likely calcite. The late vein chrysotile shows low Al_2O_3 (~ 0.5 wt%), minor contents of Ni, Mn, and rarely very low Cl. Such as in the cement chrysotile, a submicroscopic mixture with magnetite and calcite are suggested by the high FeO (~ 7 to ~ 11 wt%), and CaO (~ 0.4 wt%), respectively.

Transmission electron microscopy

For the TEM investigations of the matrix cementing the clasts, a single representative site was selected, which is highlighted by the yellow circle in Fig. 7c.

As evident from the TEM images of a representative site of the fibrous material filling the space among the breccia clasts (Fig. 12), about 90 vol% of the investigated areas shows intergrown bundles with different orientations of 'chrysotile' fibres. At a first sight, two main fibre orientations seem to be present, i.e., roughly parallel and normal to the photo plane, respectively, with the horizontal fibres that seem to wrap around the vertical ones. However, as demonstrated by Selected Area Electron Diffraction (SAED) pattern, the orientation of the chrysotile fibres is rather chaotic (Fig. 12c, d, and Fig. 13a, b). Locally, complex bundles of chrysotile

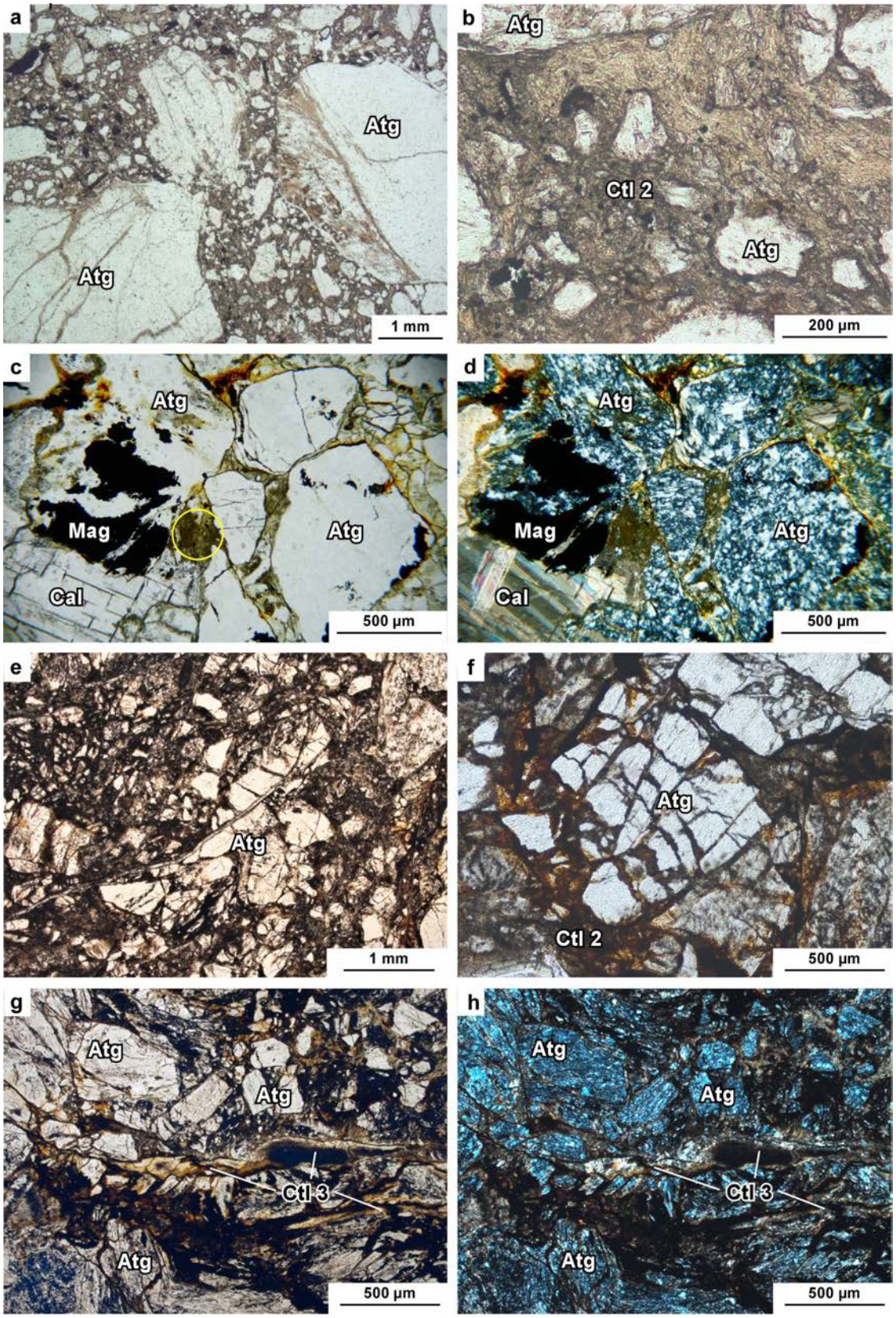

Fig. 7 - Thin section photomicrographs of representative samples of the Acquasanta Breccia. (a, b, c, e, f, g: plane polarized light - PPL; d, h: crossed polars - XP). a) representative breccia portion consisting of heterometric antigorite serpentinite clasts (Atg) surrounded by a dark material including fine to very grained antigorite clasts cemented by Ctl 2 chrysotile (sample BRA4 CP); b) detail of a) showing a portion rich in Ctl 2 chrysotile cement; c, d) Subangular fragments of antigorite serpentinite (Atg) with local black magnetite patches (Mag), included in a yellowish-brownish cement, whose nature is indistinguishable under the microscope. In the bottom left corner, a large crystal of twinned calcite (Cal) is evident. The yellow circle in c) shows the area sampled for TEM analysis (sample BRA2 CP); e) microfaults displacing elongated clasts of antigorite serpentinite (Atg) (sample AQS1); f) fragmented portions of a vein consisting of "fibrous" antigorite (Atg) (sample AQS1), surrounded by brownish Ctl2 cement; g, h) post-brecciation brittle shear zone marked by a late generation of chrysotile vein (Ctl3) (sample AQS2).

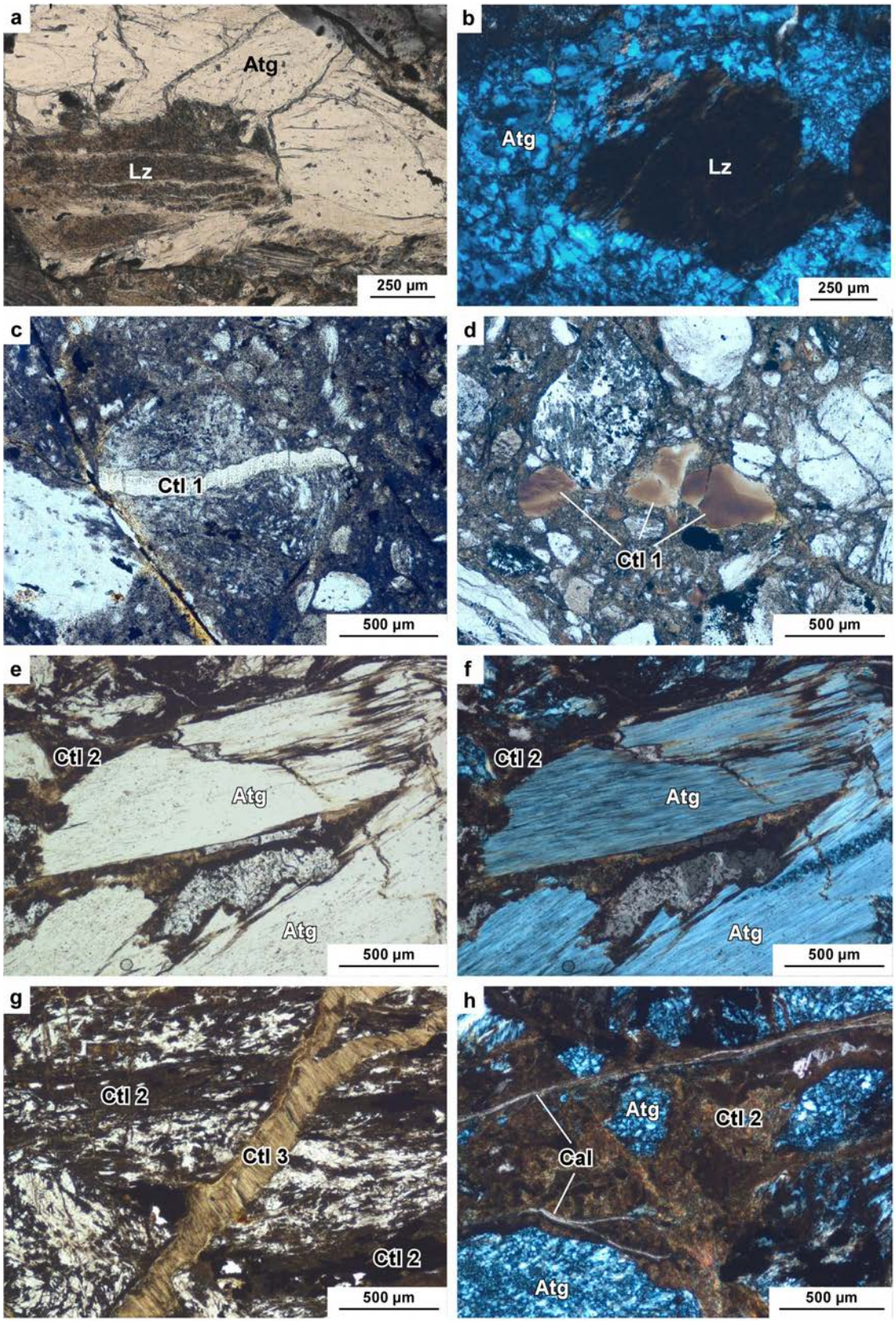

Fig. 8 - Thin section photomicrographs of representative samples of the Acquasanta Breccia. (a, c, d: PPL; b: XP). a, b) two examples of antigorite serpentinite clasts (Atg) including lizardite pseudomorphs (Lz) after original peridotite pyroxenes (a, sample CMP1; b, sample CMP2). c) antigorite serpentinite clast crossed by an early chrysotile vein (Ctl 1): Note the left margin of the clast cut by a late fracture filled with opaque iron ore (sample AQS4). d) Portion of breccia with prevailing antigorite serpentinite clasts and three clasts made up of brown vein chrysotile (Ctl 1) (sample AQS4). e, f) Fragments of antigorite veins (Atg) in the Acquasanta Breccia (sample BRA2). g) Vein of chrysotile (Ctl 3) cutting across both the clasts and the brownish cement (Ctl2) of the Acquasanta Breccia (sample BRA2). h) Thin calcite veins (Cal) crossing both the brownish cement (Ctl2) and the antigorite serpentinite clasts (Atg) (sample BRA2).

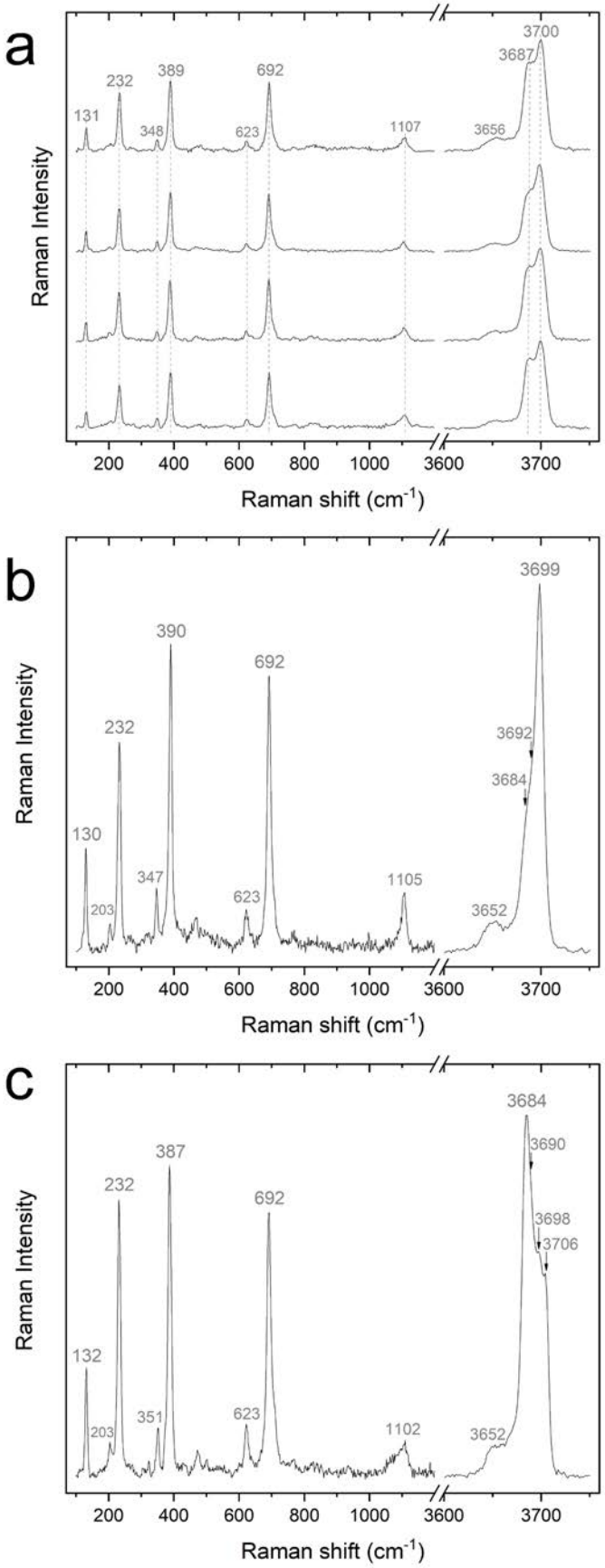

Fig. 9 - Representative Raman spectra of the yellowish-brownish cement in the 100-1200 cm^{-1} and 3600-3750 cm^{-1} regions. a) Four spectra that indicate the presence of polygonal serpentine PS-15. The shape of the lowest spectrum suggests the contribution of both chrysotile and PS-15; b) Representative spectrum of a typical chrysotile of late veins, c) Representative spectrum of a polygonal serpentine PS-30. See text for further explanations.

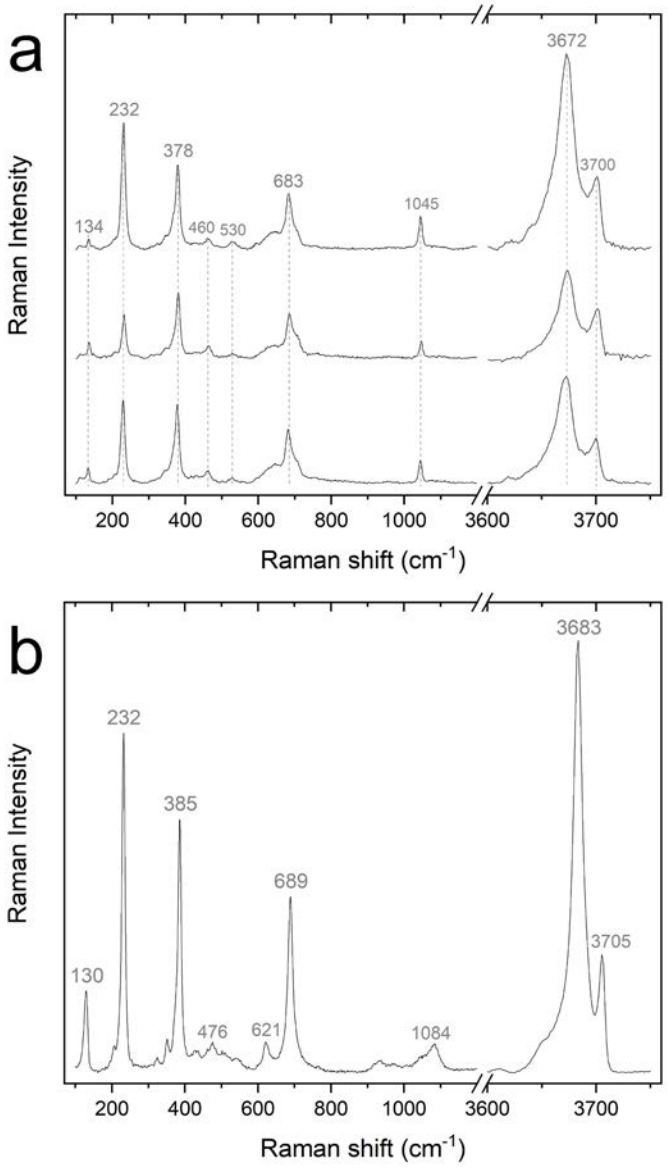

Fig. 10 - Representative Raman spectra of serpentine minerals from clasts in the 100-1200 cm^{-1} and 3600-3750 cm^{-1} regions. a) Representative Raman spectra of antigorite from three different serpentinite clasts. b) Representative spectrum of a relict lizardite preserved within some antigorite-serpentinite clasts (cf. Fig. 8a and b).

fibres appear squeezed and folded between small fragments of antigorite serpentinite (Fig. 12a) suggesting a post-crystallization deformation.

Each chrysotile fibre shows the typical scroll-like structure with a cross diameter of about 50-100 nm and length of tens of μm (possibly much longer since exceeding the area captured by the TEM). In fibres cut normal to elongation, a small hole is evident in the core, circular or elliptical in shape, commonly about 5-10 nm across. It is interesting to point out that in all TEM images the chrysotile fibres appear to form a felt surrounded by empty space, most likely originally filled by the hydrous fluid phase.

High Resolution Transmission Electron Microscopy (HRTEM) of chrysotile fibres shows mostly circular cross sections, as testified by (001) lattice fringes, but elliptical cross sections, suggesting local deformation, are widespread (Fig. 13). Even if those just described are the most recurrent features of chrysotile, fibres showing incipient polygo-

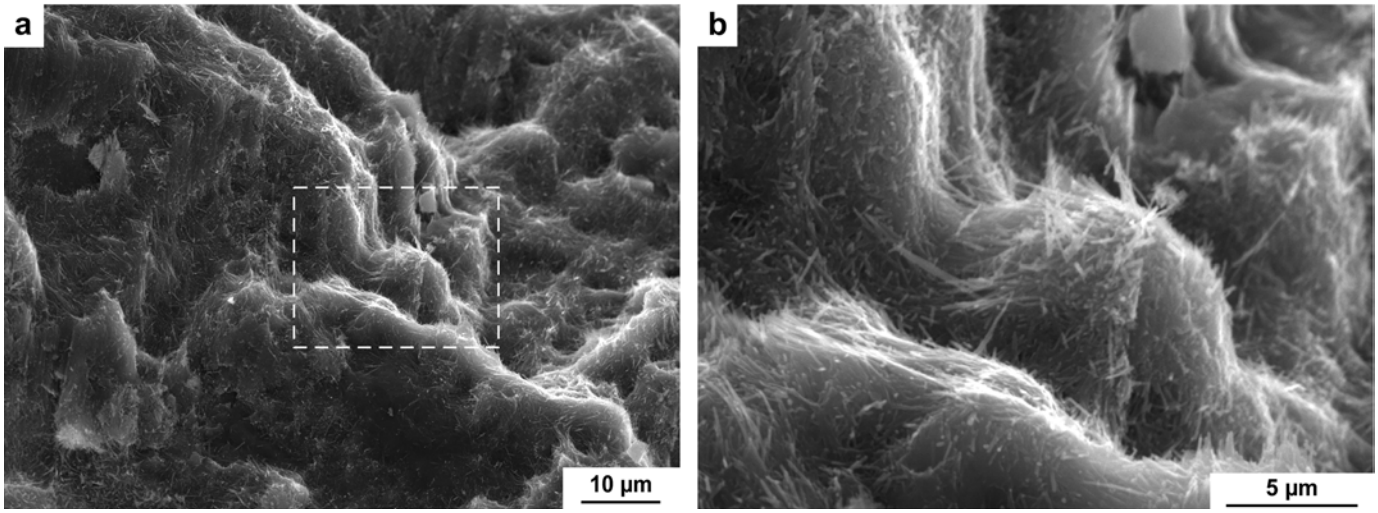

Fig. 11 - a, b) Secondary electron SEM images obtained from fresh rupture surface of the chrysotile cement (sample BRA2 CP). It is evident that the cement consists of thick bundles of very fine chrysotile fibres.

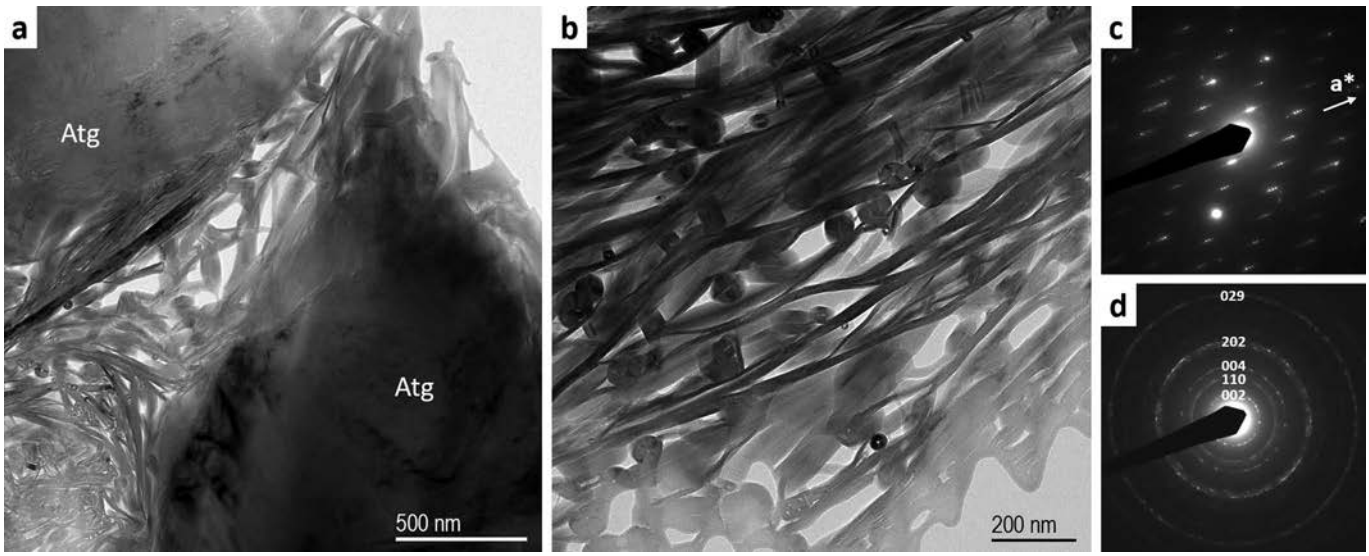

Fig. 12 - TEM images of the "chrysotile cement" (Sample BRA2 CP). a) Deformed bundle of chrysotile fibres (center) squeezed between two fragments of antigorite-serpentinite (Atg). b) Intergrown bundles with different orientations of chrysotile fibres, whose cross diameter is about 100 nm, and length tens of µm. This microstructure has been observed for about 90% of the investigated area. c) SAED pattern of antigorite showing the characteristic superstructure reflections along a*. d) SAED pattern of chrysotile showing typical rings of randomly distributed fibres. Main chrysotile reflections indexed according to the C2/m structure of Whittaker and Zussman (1956).

nalization are not infrequent (Fig. 14a). Finally, antigorite crystals passing gradually to lizardite- and chrysotile-like structures are observed (Fig. 14b). Given the great difference in both magnification and number of analysed sites between the two analytical methods, it is not surprising that the only by µ-R spectroscopy detected the local presence of PS-30 and PS-15.

DISCUSSION

Genetic mechanisms of the Acquasanta Breccia

The petrogenesis of the Acquasanta Breccia is here discussed referring to subsequent stages of the Voltri Unit tectono-metamorphic evolution (Fig. 15). The discussion is displayed referring to several geo-tectonic stages, which are preceding (Pre-Brecciation Stages), coeval (Syn-Brecciation Stages) and post-dating (Post-Brecciation Stages) the development of the Acquasanta Breccia (Fig. 16).

A - Pre-Brecciation Stages (Figs. 16a, b)

Protolith: Mantle peridotite.

Stage Pre1 - Hydration of the original mantle peridotite. Relics of early lizardite patches, most likely developed during the Mesozoic ocean-floor hydrothermal alteration (e.g., Mével, 2003), are preserved in some serpentinite clasts.

Stage Pre2 - An antigorite serpentinite formed under prograde high-pressure metamorphic conditions during the subduction stage of the Alpine orogenic cycle.

Stage Pre3 - Retrograde greenschist-facies re-equilibration

During exhumation, by combined effect of cooling and decompression, the rocks experienced a retrograde greenschist-facies re-equilibration, again in the antigorite stability field.

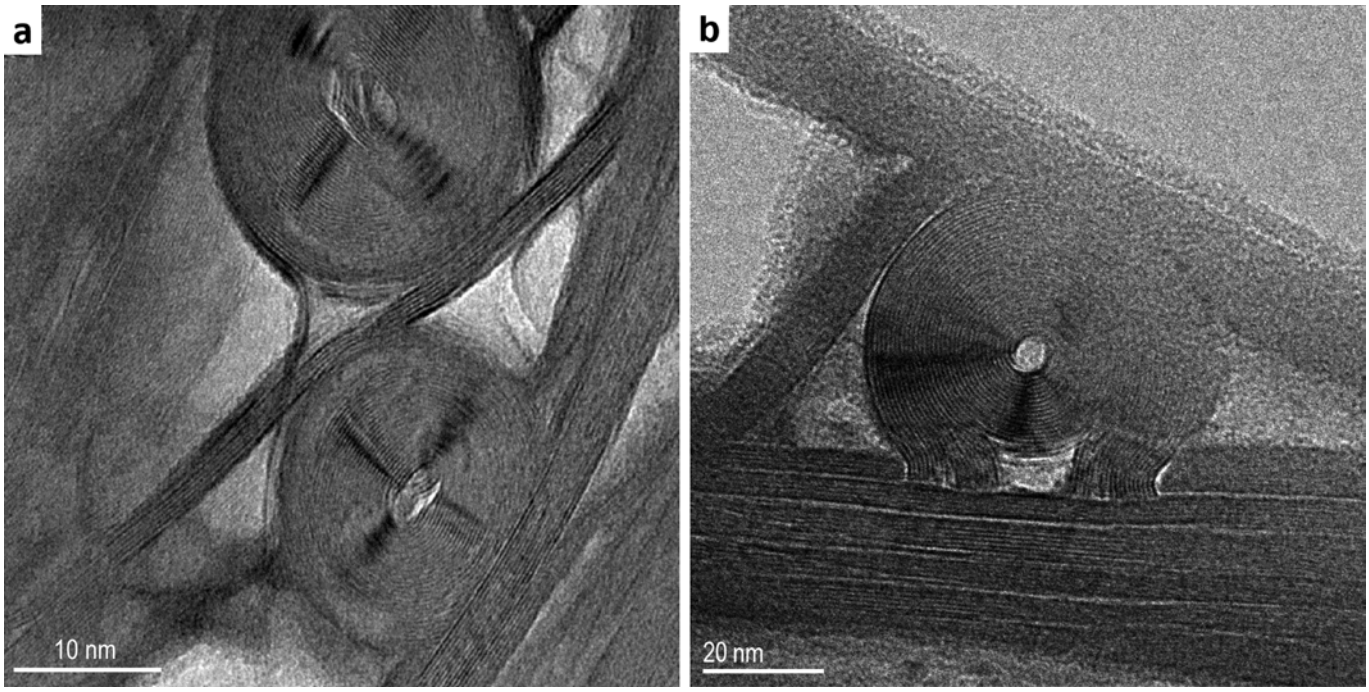

Fig. 13 - HRTEM image of the chrysotile fibres (Sample BRA2 CP). a) Chrysotile cross sections showing (001) lattice fringes in cylindrical arrangement. A thin, sinuous, longitudinal fibre crosses the field of view from the upper right to the lower left and an amorphous material (light grey) fills the space between the fibres. Note the elongated shape of the central hole in the lower chrysotile fibre due to deformation. These features characterize most of the chrysotile cement. b) Chrysotile fibre showing an uncommon structure recalling the capital Greek letter "omega".

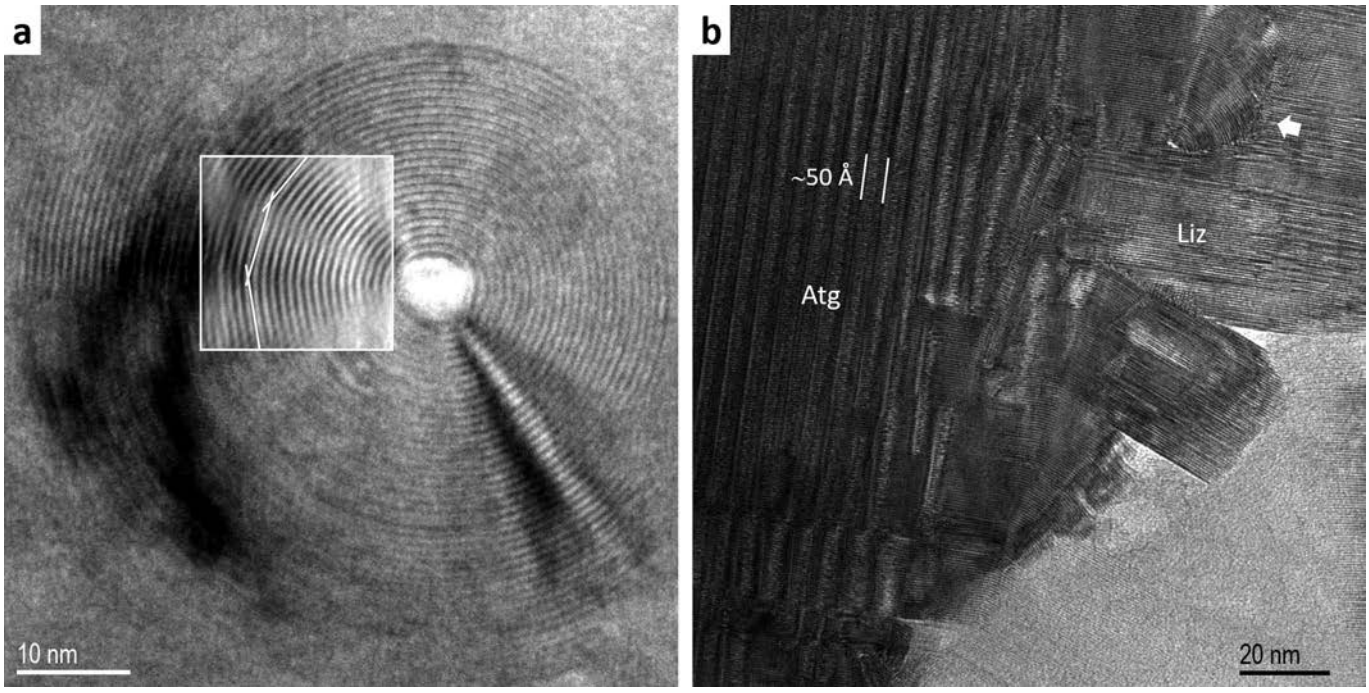

Fig. 14 - HRTEM images of the Acquasanta Breccia (Sample BRA2 CP). a) (001) lattice fringes of a chrysotile cross section showing incipient polygonalization (inset). This kind of observations on the Acquasanta Breccia cement are not infrequent. b) Lattice fringe image of the Acquasanta Breccia showing antigorite (Atg) with the typical wide (100) lattice fringes (50 Å) crosscut at high angle by (001) lattice fringes (7 Å). Note on the right, flat lizardite-like (001) fringes (Liz) and bent chrysotile-like (001) fringes (arrow). Note also how (001) fringes run with crystallographic continuity from antigorite, to lizardite to chrysotile, suggesting the formation of the latter from the former.

B) Syn-Brecciation Stages (Fig. 16c)

Last steps of the syn-exhumation tectonics

Stage Syn1 - In the final steps of exhumation, i.e., when the rocks reached shallow crustal levels within the chrysotile stability field, a widespread brecciation occurred. Brecciation was probably favoured by the homogenous mineralogy of the Acquasanta serpentinite, mostly consisting of antigorite. At shallow levels the antigorite exhibits, in response to tectonic stress, a purely brittle mechanism of deformation (Evans, 2004; Schwartz et al., 2013; Amiguet et al., 2014). The serpentinite was therefore deformed by microcrack-

ing and microfaulting. This mechanism induced a homogeneously distributed crushing that produced a cataclasite or a protocataclasite, namely a "non-foliated crackle-to-mosaic breccia" *sensu* Woodcock and Mort (2008). This structure was achieved by frictional processes that induced grain-size reduction along clast boundaries, which developed a fine-grained matrix in the interspaces between the grains. The voids were filled with hydrous fluids that are easily available at shallow depths.

Stage Syn2 - The hydrous fluid reacted with the finest more reactive antigorite clastic particles and/or neoblastic lizardite, and brought them into solution. By a dissolution-precipitation processes, a new generation of chrysotile (Ctl 2), statically grew in the voids as bundles of fibres lacking preferential orientation. As a result, a peculiar serpentinite breccia developed consisting of antigoritite clasts "cemented" by a matrix, where chrysotile (Ctl 2, Fig. 7a, b) was the dominant phase. It should be noted that chrysotile did not grow as parallel fibre of either "cross" or "slip" types in discrete veins, as commonly observed in retrograde serpentinite (e.g., Viti et al., 2014; 2018; Tesei et al., 2018). Conversely, the chrysotile filling the voids among the breccia clasts mainly crystallized as random fibers, as clearly shown by TEM images (Fig. 12). However, μ-Raman examination of many sites within this void-filling material also showed the presence of polygonal serpentine PS-15 as well (cf. Fig. 9a). These results, which are consistent with the recent data of Compagnoni et al. (2021), are not at odds with each other if the resolving power of the two techniques is considered, because the μ-Raman bean is sampling an area an order of magnitude greater than that of TEM.

C) Post-Brecciation Stages (Fig. 16d)

Late faulting and shearing occurred, and a further generation of chrysotile (Ctl 3, Fig. 8g) developed in late fractures as discrete veins cutting across both the matrix and the Acquasanta Breccia clasts (*Stage Post1*), in turn displaced by new very late fractures, individual faults and carbonate veins (*Stage Post2*) (Fig. 8h).

Geological interpretation

The Acquasanta lithotectonic unit (ALU) experienced several tectonic processes, which occurred during the exhumation history of the HP units of Voltri Unit. The dynamics of this exhumation has been interpreted in the frame of an extensional regime, which should have occurred since the late Eocene - early Oligocene (Vignaroli et al., 2008). This interpretation was based on regional-scale dynamic and kinematic models, where the orientation and magnitude of tectonic stress were related mainly to the retreat of the Alps and Apennines slab and relevant mantle flow. Alternatively, the Voltri Massif exhumation was interpreted, mostly based on field data, as the result of latest Eocene-early Miocene contractional tectonics at the Alps-Apennines junction (Capponi et al., 2009).

The emplacement of the Acquasanta Lithotectonic Unit (ALU)

The emplacement of ALU occurred during the late- to post-metamorphic evolution, i.e during the exhumation, when different orders of ductile to brittle shear zones (Hoogerduijn Strating, 1991; 1994) dissected the Voltri metamorphic com-

		Process description	Metamorphism	Index mineral	Tectonic setting
Pre-brecciation stage	STAGE PRE1	Hydration	Hydrothermal	Lizardite	Ocean spreading
	STAGE PRE2	Recrystallization	Prograde to high-pressure peak	Antigorite	Subduction
	STAGE PRE3	Recrystallization	Retrograde transition to greenschist facies	Chrysotile (Ctl1) ± lizardite	Exhumation
Brecciation stage	STAGE SYN1	Pervasive cataclasis, development of the Acquasanta Breccia	Sub-greenschist facies to anchizone (?)	Chrysotile (Ctl2)	Late exhumation stage
	STAGE SYN2	Growth of chrysotile fibre-bundles between the breccia clasts	Sub-greenschist facies to anchizone (?)	Chrysotile (Ctl2)	Late exhumation stage
Post-brecciation stage	STAGE POST1	Development of a network of individual faults and related fault breccias	None, development of individual chrysotile veins	Chrysotile (Ctl3)	Individuation of the main fault-bounded lithotectonic units
	STAGE POST2	Development of faults at very shallow crustal levels	None, development of individual carbonate veins	Calcite	Final setting of present lithotectonic units

Fig. 15 - Main petrogenetic and tectonic stages that affected the Acquasanta lithotectonic unit and led to the formation of an original antigorite serpentinite, successively exhumed and re-equilibrated under greenschists facies conditions and then pervasively fractured (Acquasanta Breccia) in the intermediate to late exhumation stages. The Acquasanta Breccia were then displaced by more recent fault systems.

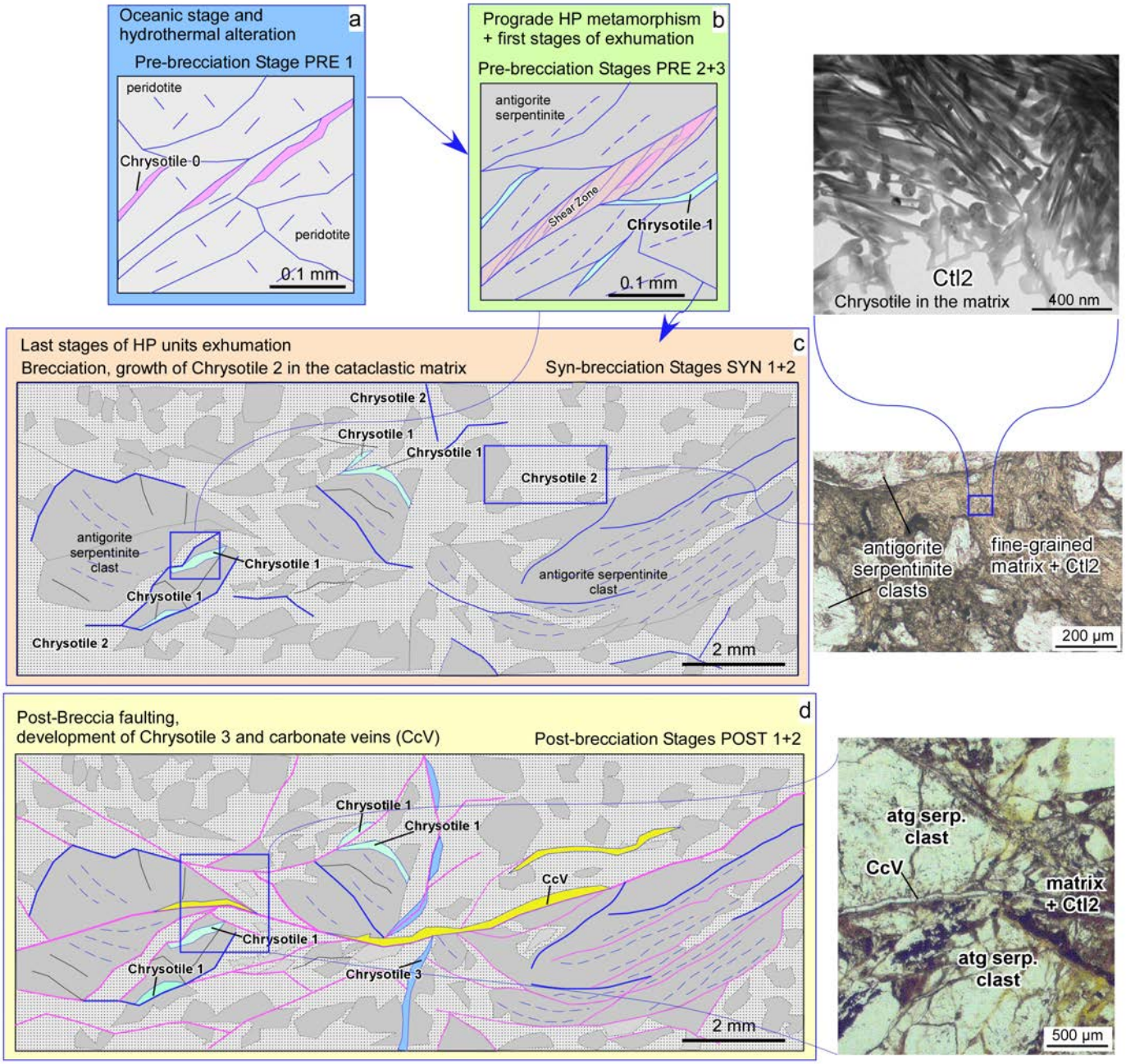

Fig. 16 - Interpretative sketch of the genetic mechanism of the Acquasanta Breccia. See section "Genetic mechanisms of the Acquasanta breccia" for explanation. Blue lines indicate fractures formed before and during the brecciation stage, while red lines indicate the microfaults developed during the late faulting stages. Light blue filled fractured indicate chrysotile 1 veins, Blue filled fractures indicate chrysotile 3 veins. Atg: antigorite; Ctl: chrysotile; CcV: carbonate veins.

plex. The ALU tectonic setting was then ultimately defined by individual faults, which clearly displaced the composite metamorphic foliation, as described in Sections 3 and 5.2.3.

The main tectonic foliation that can be recognized at regional scale in the Voltri Unit- and consequently in the ALU - is coeval with the retrograde metamorphism connected to the exhumation of the unit (Capponi and Crispini, 2008). Such a foliation should have developed during the late Eocene (Hoogerdujin Strating, 1991) and ended later than about 33 Ma (Federico et al., 2005). A composite metamorphic foliation, resulting from the superposition of two main folding events and mainly referable to greenschist-facies conditions, transposed the primary lithological contacts (Hoogerdujin Strating, 1991; Capponi and Crispini, 2008) between serpentinite, metabasite and peridotite. During this retrograde metamorphic phase (Stage Pre3), the first generation of chrysotile (Ctl1) developed. The development of the Acquasanta Breccia occurred after the onset of the greenschist-facies, as discussed below.

The genesis of the Acquasanta breccia within ALU

It is generally accepted in literature that the tectonic evolution of the meta-ophiolites complexes (e.g., the Voltri Massif) during subduction and exhumation processes is mostly driven by localization of shearing controlled mainly by the rheology of the serpentinite layers rather than that of peridotite and basalts (see, for the Voltri Massif: Hoogerduijn Strating, 1991). According to recent interpretation (Malatesta et al., 2012), the Voltri Massif exhumation could have occurred inside an inverted subduction channel, resulting in

a tectonic mélange in the sense of Guillot et al. (2009) and Festa et al. (2010), where the foliated serpentinite played a crucial role in the mechanics of shearing and faulting. The foliated serpentinite act as a "soft matrix" of the more competent metabasites, massive serpentinites and peridotites that were dynamically decoupled during exhumation and acted as quasi-rigid objects. Indeed, the Voltri Unit consists of different lithotypes with very contrasting mechanical properties: slices of massive peridotite, km-scale tectonic units of metabasite, massive serpentinite bodies and foliated serpentinite layers, metasediment successions (mostly calc-schist interbedded with micaschist). In such a heterogeneous complex, the propagation of thrusts and faults at shallow crustal levels can be impeded, locally, by mechanical factors such as poor lateral continuity or paucity of potentially weak layers suitable for the localization of deformation and the progressive increase of tectonic slip magnitude. Consequently, when the value of the strain rate significantly varies within heterogeneous fault zones and tectonic slices, and the deformation cannot be completely localized along weak layers and individual shear zones, strong mechanical instabilities and faulting are likely to occur also within the more competent rock lenses (Fagereng and Sibson, 2010; Collettini et al., 2011). In these cases, distributed cataclastic crushing (microcracking and microfaulting) of varying intensity may occur over broad areas, even far from the main fault, as displacement along the main slip surfaces is impeded (Sibson, 1986).

A cataclastic process, such as the one described above, is envisaged for the origin of the Acquasanta Breccia. A cataclastic deformation, i.e., a combination of frictional wear and grain cataclasis, associated with separation of grains by shear and followed by a growth of chrysotile bundles in the matrix microvoids, promoted the formation of the breccia. The propagation of the shear zones bounding the ALU during the exhumation process could have been partially impeded by the presence of adjoining rigid peridotite mass (such as those of the Bric Boessa Unit), and the scarce lateral continuity of weak calc-schist layers. This could have allowed a marked strain partitioning and promoted a distributed cataclasis over large parts of ALU, except for those consisting of prevalent metabasite.

The brecciation of ALU serpentinites then occurred by progressive, cataclastic grain-size reduction, and allowed syn- to post-tectonic fluids to penetrate the rocks, enhancing the static growth of chrysotile (Ctl2) at the expense of both the fine-grained antigorite clasts, which locally preserve older Ctl1 veins, and the neoblastic lizardite. The highly porous fabric of the breccia, characterized by a network of interconnected microvoids, favoured the influx of hydrous fluids that impregnated the rock favouring dissolution of the finest and most reactive micro- to nano- antigorite fragments developed at the expense of the antigorite serpentinite clasts. Consequently, the chrysotile started to grow under static conditions forming a network of fibre bundles, intimately interconnected. A dissolution-precipitation process could have been the predominant deformation mechanism for the chrysotile growth, as frequently observed in serpentinites at relatively low- temperature (Andreani et al., 2005; Hirauchi and Yamaguchi, 2007; Viti et al., 2018).

The later tectonic stages of ALU

After the development of the Acquasanta Breccia, the tectonic evolution of ALU continued at shallower crustal levels, probably during the juxtaposition of the very-low grade tectono-metamorphic units of the Sestri-Voltaggio Zone with the Voltri Massif. During these late deformation stages, a new generation of chrysotile (Ctl 3) formed in cross-cutting veins displaying a crack-seal texture, thus suggesting the precipitation of the minerals during incremental fault movements. Finally, another brittle deformation stage occurred, mostly characterized by cataclasis and cataclastic flow sustained by carbonate fluids. In this case, the deformation was confined only along the very late faults and brittle shear zones that, in the study area, presently bounds different-order tectonic slices of the eastern Voltri, Palmaro-Caffarella and Sestri-Voltaggio units.

CONCLUSIONS

A detailed geological and mineralogical study of a peculiar serpentinite breccia (Acquasanta Breccia) exposed in the eastern Voltri Massif highlights the importance of the compositional and structural heterogeneities within ophiolite-bearing exhumation channels. In serpentinites, and particularly in the serpentinite matrix of a exhumation channel mélange, diffuse brittle fracturing is thought to be an unusual process during retrogression (e.g., Viti et al., 2018), since the semi-brittle to brittle deformation mostly results in the formation of layers of incohesive gouge along faults and layers of oriented serpentine minerals (typically chrysotile) in shear zones (Andreani et al., 2005; Hirauchi and Yamaguchi, 2007; Hirth and Guillot, 2013). Fracturing and cataclasis are thought to occur mainly near late faults, along which new generation of serpentine minerals can grow in the relevant vein networks (e.g., Hoogerdujin Strating and Vissers, 1994; Groppo and Compagnoni, 2007).

In our case of a 10 km-scale serpentinite tectonic slice (ALU) sandwiched between a mélange zone (Leira Unit) and a more competent tectonic slice (Bric Boessa Unit), diffuse brittle fracturing occurred indeed prior to the very late faulting stages, during the intermediate to late stages of the Alpine exhumation. Although pervasive brittle deformation of serpentinite is expected to occur mainly during prograde metamorphism, when antigorite is undergoing brittle to ductile transition (Guillot et al., 2015), the Acquasanta breccia conversely formed later in the history, after the development of the regional greenschist-facies antigorite foliation, namely during the retrograde exhumation stages under semi-brittle conditions. This process was favoured by the high lithological heterogeneity of the boundary zone between the Voltri and the Palmaro-Caffarella units. There, the Leira "mélange zone" in the ALU hangingwall, which consists of metabasite bodies "floating" in a tectonic matrix made up of metasediments, and the poorly serpentinized peridotite of the Bric Boessa Unit in the footwall, did play an important role for the development of pervasive brecciation at the expense of the ALU more competent rock bodies, where fracturing and cataclasis involved large rock volumes due to the difficulty in the localization of shearing.

High differences in the rheological behaviour of massive metagabbro, massive serpentinite, or peridotite bodies compared to the foliated serpentinite matrix was already highlighted by Malatesta et al. (2012), who suggested for the Voltri Massif an important tectonic decoupling not only during subduction but also during the exhumation process.

Our observations highlight the important role of the compositional and structural heterogeneities in generating abrupt changes of the deformation mechanisms within ophiolite-bearing exhumation channels. This conclusion is valid re-

gardless of the interpretation that the Voltri Massif was generated by a tectonic mixing in a (subduction-) exhumation channel (in the sense of Festa et al., 2010; 2019), as suggested by Malatesta et al. (2012) or conversely as the result of non-chaotic progressive shearing, as tectonic does not seems to be an efficient mixing process at shallow structural levels (Festa et al., 2022).

Therefore, it can be concluded that the Acquasanta Breccia is not a trivial fault rock, but instead it is a peculiar type of breccia recording a poorly known intermediate step of the exhumation process. We presume that other similar occurrences could be found, maybe in other collisional belts, by detailed geological and mineralogical investigations.

ACKNOWLEDGEMENTS

This work represents a scientific improvement of some of the studies performed in 2017 and 2018 for the setting up of the geoenvironmental model of the "Gronda di Genova" highway by-pass of Genova city, Italy, commissioned by Autostrade per l'Italia S.p.A. (ASPI, Rome) to the "G. Scansetti" Interdepartmental Center for Studies on Asbestos and other toxic particulates of the University of Torino (Italy), the Institute of Geosciences and Earth Resources of the National Research Council of Italy (CNR), Torino, and Gi-RES srl (CNR spinoff company), Torino. Francesco Cipolli (Tecne S.p.A, Genova), Vittorio Boerio and Simona Polattini (Tecne S.p.A, Milano) are kindly acknowledged for making subsurface data available. Marcello Mellini is thanked for helpful discussions and suggestions.

The authors are very indebted to Associate Editors J. A. Padrón-Navarta and Y. Dilek, for the helpful advices and constructive comments that significantly improved the manuscript. The suggestions of two anonymous reviewers motivate us to describe with greater detail some essential topics.

Micro-Raman spectra have been obtained with the equipment acquired by the Interdepartmental Centre "G. Scansetti" for Studies on Asbestos and Other Toxic Particulates (University of Torino) with a grant from Compagnia di San Paolo, Torino, Italy.

Authors' contribution:

L. Barale, R. Compagnoni and F. Piana conceived the paper, worked on field and lab, wrote and made the revision of text and figures. S. Tallone largely contributed to the field work and mapping, S. Botta made a part of the petrographic analyses, G. Capitani performed TEM analysis, R. Cossio and J. R. Petriglieri performed Micro-Raman analysis, C. Avataneo and F. Turci performed SEM analysis. I. Marcelli managed the CNR IGG geodatabase used to realise the presented geological map and cross-sections.

REFERENCES

Amiguet E., van de Moortèle B., Cordier P., Hilairet N. and Reynard B., 2014. Deformation mechanisms and rheology of serpentines in experiments and in nature. J. Geophys. Res. Solid Earth, 119 (6): 4640-4655.

Andréani M., Boullier A.M. and Gratier J.P., 2005. Development of schistosity by dissolution-crystallization in a Californian serpentinite gouge. J. Struct. Geol., 27 (12): 2256-2267.

Barale L., Piana F., Compagnoni R., Tallone S., Avataneo C., Botta S., Marcelli I., Irace A., Mosca P., Cossio R. and Turci F., 2020. Geological Model for naturally occurring asbestos content prediction in the rock excavation of a long tunnel ("Gronda di Genova" Project, NW Italy). Environ. Engin. Geosci., 26 (1): 107-112.

Barale L., Petriglieri J.R., Botta S. and Piana F., 2022. Low-temperature, diagenetic serpentinization of peridotite clasts in lower Miocene marine conglomerates, Torino Hill, NW Italy. Mar. Petrol. Geol., 143: 105830.

Bernoulli D., Caron C., Homewood P., Kälin O. and Van Stuijvenberg J., 1979. Evolution of continental margins in the Alps. Schweiz. Miner. Petrogr. Mitt., 59: 165-170.

Botta S., Avataneo C., Barale L., Compagnoni R., Cossio R., Marcelli I., Piana F., Tallone S. and Turci F., 2020. Petrofacies for the prediction of NOA content in rocks: application to the "Gronda di Genova" tunneling project. Bull. Engin. Geol. Environ., 79: 185-204.

Capponi G. and Crispini L., 2008. Note illustrative della Carta Geologica d'Italia alla scala 1:50.000. Foglio 213-230 Genova. SELCA, Firenze, 139 pp.

Capponi G., Crispini L., Federico L. and Malatesta C., 2016. Geology of the Eastern Ligurian Alps: a review of the tectonic units. It. J. Geosci., 135 (1): 157-169.

Capponi G., Crispini L., and Scambelluri M., 2009, Comment on "Subduction polarity reversal at the junction between the Western Alps and the Northern Apennines, Italy", by G. Vignaroli, C. Faccenna, L. Jolivet, C. Piromallo and F. Rossetti. Tectonophysics, 465: 221-226.

Cashman S.M. and Whetten J.T., 1976. Low temperature serpentinization of peridotite fanglomerate on the west margin of the Chiwaukum graben, Washington. GSA Bull., 87 (12): 1773-1776.

Chiesa S., Cortesogno L., Forcella F., Galli M., Messiga B., Pasquaré G., Pedemonte G.M., Piccardo G.B. and Rossi P.M., 1975. Assetto strutturale ed interpretazione geodinamica del gruppo di Voltri. Boll. Soc. Geol. It., 94: 555-581.

Collettini C., Niemeijer A., Viti C., Smith S.A.F. and Marone C., 2011. Fault structure, frictional properties and mixed-mode fault slip behavior. Earth Planet. Sci. Lett., 31 (3-4): 316-327.

Compagnoni R., Cossio R. and Mellini M., 2021. Raman anisotropy in serpentine minerals, with a caveat on identification. J. Raman Spectr., 52: 1334-1345.

Cortesogno L. and Haccard D., 1984. Note illustrative alla Carta geologica della zona Sestri - Voltaggio. Mem. Soc. Geol. It., 28: 115-150.

Craw D., Landis C.A., and Kelsey P.I., 1987. Authigenic chrysotile formation in the matrix of Quaternary debris flows, Northern Southland, New Zealand. Clays Clay Miner., 35: 43-52.

Crispini L. and Capponi G., 2001. Tectonic evolution of the Voltri Group and Sestri Voltaggio Zone (southern limit of the NW Alps): a review. Ofioliti, 26 (2): 161-164.

Evans B.W., 2004. The Serpentinite Multisystem Revisited: Chrysotile is Metastable. Int. Geol. Rev., 46 (6): 479-506.

Fagereng A. and Sibson R.H., 2010. Mélange rheology and seismic style. Geology, 38: 751-754.

Federico L., Capponi G., Crispini L. and Scambelluri M., 2004. Exhumation of Alpine high-pressure rocks: insights from petrology of eclogite clasts in the Tertiary Piedmontese basin (Ligurian Alps, Italy). Lithos, 74: 21-40.

Federico L., Capponi G., Crispini L., Scambelluri M. and Villa I.M., 2005. ^{40}Ar-^{39}Ar dating of high-pressure rocks from the Ligurian Alps: evidence for a continuous subduction - exhumation cycle. Earth Planet. Sci. Lett., 240 (3-4): 668-680.

Festa A., Barbero E., Remitti F., Ogata K. and Pini G.A., 2022. Mélanges and chaotic rock units: Implications for exhumed subduction complexes and orogenic belts. Geosyst. Geoenvir., 1 (2): 100030.

Festa A., Pini G.A., Dilek Y. and Codegone G., 2010. Mélanges and mélange-forming processes: a historical overview and new concepts: Intern. Geol. Rev., 52: 1040-1105.

Festa A., Pini G.A., Ogata K. and Dilek Y. 2019. Diagnostic features and field-criteria in recognition of tectonic, sedimentary and diapiric mélanges in orogenic belts and exhumed subduction-accretion complexes. Gondwana Research, 74, 7–30.

Groppo C. and Compagnoni R., 2007. Metamorphic veins from the serpentinites of the Piemonte ZoneWestern Alps, Italy: A review. Per. Miner., 76 (3): 127-153.

Groppo C., Rinaudo C., Cairo S., Gastaldi D. and Compagnoni R., 2006. Micro-Raman spectroscopy for a quick and reliable identification of serpentine minerals from ultramafics. Eur. J. Miner., 18: 319-329.

Guillot S., Hattori K., Agard P., Schwartz S. and Vidal O., 2009. Exhumation processes in oceanic and continental subduction contexts: a review. In: S. Lallemand and F. Funiciello (Eds.), Subduction zone geodynamics. Springer-Verlag, Berlin Heidelberg, p.175-206.

Guillot S., Schwartz S., Reynard B., Agard P. and Prigent C., 2015. Tectonic significance of serpentinites. Tectonophysics, 646: 1-19.

Hirauchi K.I., 2006. Serpentinite textural evolution related to tectonically controlled solid-state intrusion along the Kurosegawa Belt, northwestern Kanto Mountains, central Japan. Isl. Arc, 15 (1): 156-164.

Hirauchi K. and Yamaguchi H., 2007. Unique deformation processes involving the recrystallization of chrysotile within serpentinite: implications for aseismic slip events within subduction zones. Terra Nova, 19: 454-461.

Hirth G. and Guillot S., 2013. Rheology and tectonic significance of serpentinite. Elements, 9 (2): 107-113.

Hoogerduijn Strating E.H., 1991. The evolution of Piedmont Epi-Ligurian Ocean: A structural study of ophiolites complexes in Liguria (NW Italy), PhD Thesis, Univ. Utrech, Geol. Ultraiect., 74, 211 pp.

Hoogerduijn Strating E.H., 1994. Extensional faulting in an intra-oceanic subduction complex; working hypothesis for the Palaeogene of the Alps-Apennine system. Tectonophysics, 238 (1-4): 255-273.

Hoogerduijn Strating E.H. and Vissers R.L.M., 1994. Structures in natural serpentinite gouges: J. Struct. Geol., 16: 1205-1215.

Malatesta C., Crispini L., Federico L., Capponi G. and Scambelluri M., 2012. The exhumation of high-pressure ophiolites (Voltri Massif, Western Alps): Insights from structural and petrologic data on metagabbro bodies: Tectonophysics, 568-569: 102-123.

Mével C., 2003. Serpentinization of abyssal peridotites at mid-ocean ridges. C.R. Geosci., 335 (10-11): 825-852.

Petriglieri J.R., Salvioli-Mariani E., Mantovani L., Tribaudino M., Lottici P.P., Laporte-Magoni C. and Bersani D., 2014. Micro-Raman mapping of the polymorphs of serpentine. J. Raman. Spectrosc., 46: 953-958.

Rinaudo C., Gastaldi D. and Belluso E., 2003. Characterization of chrysotile, antigorite and lizardite by FT-Raman spectroscopy. Can. Miner., 41: 883-890.

Rovereto G., 1939. Liguria Geologica. Mem. Soc. Geol. It., 2: 1-768.

Rubatto D. and Scambelluri M. 2003. U-Pb dating of magmatic zircon and metamorphic baddeleyite in the Ligurian eclogites (Voltri Massif, Western Alps). Contrib. Miner. Petrol., 146: 341-355.

Sacco F., 1889-1890. Il Bacino Terziario e Quaternario del Piemonte. Tip. Bernardoni, Milano.

Schwartz S., Guillot S., Reynard B., Lafay R., Debret B., Nicollet C., Lanari P. and Auzende A.L., 2013. Pressure-temperature estimates of the lizardite/antigorite transition in high pressure serpentinites. Lithos, 178: 197-210.

Sibson R.H., 1986. Brecciation processes in fault zones: inferences from earthquake rupturing. Pure Appl. Geophys., 124: 159-175.

Tesei T., Harbord C.W.A., Paola N.D., Collettini C. and Viti C., 2018. Friction of mineralogically controlled serpentinites and implications for fault weakness. J. Geophys. Res. Solid Earth, 123: 6976-6991.

Vanossi M., Cortesogno L. Galbiati B. Messiga B., Piccardo G. and Vannucci R. 1984, Geologia delle Alpi Liguri: Dati, problemi, ipotesi, Mem. Soc. Geol. Ital., 28: 5-75.

Vignaroli G., Faccenna C., Jolivet L., Piromallo C. and Rossetti F., 2008. Subduction polarity reversal at the junction between the Western Alps and the Northern Apennines, Italy. Tectonophysics, 450: 34-50.

Vignaroli G., Faccenna C., Jolivet L., Piromallo C. and Rossetti F., 2009. Reply to the comment by G. Capponi et al. on "Subduction polarity reversal at the junction between the Western Alps and the Northern Apennines, Italy", by G. Vignaroli et al. (Tectonophysics, 2008, 450: 34-50). Tectonophysics, 465: 227-231.

Vignaroli G., Rossetti F., Rubatto D., Theye T., Lisker F. and Phillips D., 2010. Pressure-temperature-deformation-time (P-T-d-t) exhumation history of the Voltri Massif HP complex, Ligurian Alps, Italy. Tectonics, 29: TC6009.

Viti C., Collettini C. and Tesei T., 2014. Pressure solution seams in carbonatic fault rocks: mineralogy, micro/nanostructures and deformation mechanism. Contrib. Miner. Petrol., 167: 970.

Viti C., Collettini C., Tesei T., Tarling M.S. and Smith S.A.F., 2018. Deformation processes, textural evolution and weakening in retrograde serpentinites. Minerals, 8: 241.

Whittaker E.J.W., and Zussman J., 1956. The characterization of serpentine minerals by X-ray diffraction. Miner. Mag., 31: 107-126.

Woodcock N.H. and Mort K., 2008. Classification of fault breccias and related fault rocks. Geol. Mag., 145 (3): 435-440.

Received, December 23, 2022
Accepted, March 15, 2023
First published online, March 28, 2023